

DAMPING CHARACTERISTICS OF MONTMORILLONITE BASED POLYESTER/CLAY NANOCOMPOSITES

R.Velmurugan* and K. Karthikeyan*

Abstract

This work presents the experimental study of free vibration and damping characteristics of Polyester/Clay Nanocomposites (PCN). PCN are prepared by dispersing Un-modified Montmorillonite clay (UMT) and organically modified Montmorillonite clay (MMT) in polyester resin and subsequently cross-linked using Methyl Ethyl Keton Peroxide (MEKP) catalyst at different clay concentrations (1,2,3, and 5Wt. %). The X-ray diffraction (XRD) and Transmission Electron Microscopy (TEM) show the increasing interlayer d-spacing of both UMT and MMT which indicates the intercalated composites. Tensile test result shows that the tensile strength and modulus are increased by 55% and 43% for 5Wt % of MMT clay concentration respectively. The impact energy and heat deflection temperatures are increased by 68.27% and 25% for MMT clay respectively. The DMA studies reveal that the storage and loss modulus are increasing monotonically with increase of clay concentration. The Impulse technique and Logarithmic decrement method are used in experimental modal analysis and it is seen that increase of Wt. % of clay in polyester matrix increases the natural frequency and damping characteristics of MMT.

Keywords: *Un-modified Montmorillonite clay (UMT), Organically Modified Montmorillonite clay (MMT), Natural frequency and Damping factor*

Introduction

It has been proved in recent years that polymer reinforced with less amount of nano-scale clay particles (<5%) can significantly improve the mechanical, thermal, and barrier properties of the pure polymer matrix [1-2] and are light in weight.

Recent studies reveal that nano clay composites dispersed in polymer matrix exhibit dramatic improvement in stiffness, strength, dimensional stability, improved flame retardancy, improved solvent and UV resistance. These materials also provide reduction in permeability to gases [3], improve thermal stability [4], and good ablative properties [5]. These property improvements occur at extremely low concentration of the aluminosilicates (1–5 Vol.%) compared to conventional filler material in a polymer (20-30%).

Montmorillonite is a crystalline material consisting of number of 1nm thick layers (or sheets) which are made of an octahedral sheet of alumina fused into two tetrahedral sheets of silica. Nanoscale layered clays with high aspect ratio and high strength play an important role in forming intercalation/exfoliation polymer nanocomposites [6].

Kornmann et al. [7] reported the dispersion of Montmorillonite in unsaturated polyester resin and found that the fracture toughness was doubled by dispersing 1.5 % (by volume) of aluminosilicates. Suh et al. [8] demonstrated that the resulting properties of polyester clay nanocomposites were mainly dependent upon mixing of the clay with polyester resin promoters as well as the curing conditions. Bharadwaj et al. [9] showed that the tensile modulus and oxygen permeability rate have decreased with increasing clay content. Recently Baran Inceoglu and Ulku Yilmazer [10] synthesized the un-saturated polyester based

* Department of Aerospace Engineering and Composites Technology Centre, Indian Institute of Technology Madras
Chennai-600 036, India E-mail: rvel@aero.iitm.ernet.in

Manuscript received on 26 Jul 2005; Paper reviewed, revised and accepted on 17 Oct 2005

nanocomposites with organically treated Na-Montmorillonite (Cloisite 30B) and non-treated Na-Montmorillonite (Cloisite Na⁺) clays. The Tensile, flexural, and impact strength of composites with modified Montmorillonite were higher than the unmodified Montmorillonite. It was concluded that the exfoliation was well formed in the modified Montmorillonite content.

Engineering structures are generally designed for strength. Stability and vibration are also very important, especially when the structural elements are thin and subjected to dynamic loads. Since weight is a crucial factor in aircraft structures, the use of conventional isotropic material gives very little room for weight savings. Unlike in isotropic materials, the properties of composite materials can be tailored to have high strength and less weight. As the strength-to-weight ratio of composite materials is high, structures made of composites often become very thin. Adjustment in the natural frequency of isotropic material is done either by changing the thickness or adjusting the boundary conditions. The dynamic characteristic of layered composite materials has also been studied by many authors [11-14].

However not much work is done on studies of the natural frequency and damping factor of PCN. Therefore, it is decided to study the dynamic characteristics of PCN as it has lot of potential in strength critical applications.

In the present work, we have carried out experiments on the prediction of mechanical properties of PCN with respect to different type of clay and different Wt. % of clay. The dynamic characteristics such as natural frequency, damping factor and Loss tangent for different Wt. % of clay and different type of clay are studied. Since there is no well established theoretical modeling for the prediction of natural frequency and damping factor, the conventional method has been used to find the natural frequency theoretically. Good agreement of theoretical results with the experiment is found in most of the cases.

Experimental Details

Materials

The UMTand MMT clay from southern clay products, Texas, were used as the reinforcing fillers. High styrene content Isophthalic general-purpose polyester resin from Sakthi fibers, India, was used as

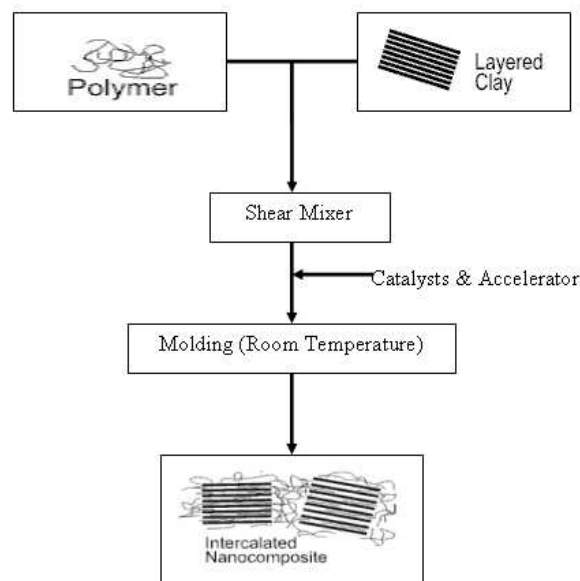


Fig. 1 Schematic methodology used in this study

matrix in order to have better diffusion into the galleries of Montmorillonite. Methyl Ethyl Ketone Peroxide (MEKP) was used as the catalyst. Cobalt nophanate was used as accelerator. The quantity of accelerator and catalyst were ~1.5Vol% of the resin.

Preparation of PCN

The schematic representation of the methodology used for the preparation of PCN is shown in Fig. 1. The synthesis of nanocomposites involves the dispersion of UMTand MMT clay for different Wt. % (1, 2 3, and 5Wt. %). After adding the desired amount of clay into the polyester resin, the mixture was stirred by laboratory mechanical stirrer, rotating with 2000rpm for 10hrs. The increase of mixing time increased the viscosity of the resin-clay mixer and the vicinity of air bubbles was reduced. The degassing of the mixer was done for 1hr and the 1.5 .% by weight of MEKP was added to the pre-mixer to initiate the cross-linking and then cobalt nophanate accelerator was added to the mixer for curing. The 30cmX30cmX0.3cm resin casting sample was obtained for every Wt. % of clay and the specimens were cut from the samples for testing.

Characterization and Property Evaluation

The X-Ray Diffraction was performed on UMTand MMT clay cured samples to evaluate the degree of intercalation and the d – spacing between the platelets.

It was carried out with a scanning rate of 2°/min and CuK α radiation at 30KV and 15mA ($\lambda = 1.5406\text{\AA}$). Thin foils of 100-200nm thick specimen were made for Transmission Electron Microscopy (TEM) using Phillips electron microscopy operating at 200KV.

Tensile test was performed on the Instron machine (4301) with cross head speed of 1mm/min according to the ASTM D638. The Izod impact test was conducted to study the impact energy according to the ASTM D256. Heat deflection temperature was obtained by ASTM D648. The Dynamic Mechanical Analysis (DMA) results were obtained using NETZSCH DMA242 C Thermal Analyzer/Dynamic Mechanical Analyzer (DMA) system at frequency rate of 10Hz. This system measures the storage modulus and loss tangent ($\tan \delta$) of the material.

Modal Testing

Modal testing was carried out to study the vibrational characteristics of the nanocomposite specimens. This study was used for the comparison of modal properties, calculation of damping, structural modification and optimization and force calculations.

PCN beam specimens were prepared for different concentration of UMT and MMT clay. The size of the specimen was 200mmx20mmx3mm. The first four modes of natural frequencies were obtained by considering the specimens as cantilever beam by using Impulse Technique. Impulse Technique and logarithmic decrement were used to compute the damping factor of beam specimens.

Analysis

By considering the nanoclay composites as quasi-isotropy the natural frequency of the cantilever beams is obtained as follows.

The equation of motion of Euler-Bernoulli for beam is,

$$m(x) \left(\frac{\partial^2 w}{\partial t^2} \right) + c \left(\frac{\partial w}{\partial t} \right) + EI \left(\frac{\partial^4 w}{\partial x^4} \right) = f(x,t) \quad (1)$$

where, m is mass per unit length of the beam defined as $m = \rho A$. If no damping and external force is considered then $c = 0$, $f(x,t) = 0$. By assuming

$EI(x)$ and $m(x)$ as constant, the equation (1) can be rewritten as,

$$\left(\frac{\partial^2 w}{\partial t^2} \right) + \frac{EI}{m} \left(\frac{\partial^4 w}{\partial x^4} \right) = 0 \quad (2)$$

Assuming steady state vibration in harmonic form, we have

$$w(x,t) = W(x) * \sin(\omega t - \phi) \quad (3)$$

Substituting equation (3) in (2),

$$\left(\frac{\partial^4 W(x)}{\partial x^4} \right) - \beta^4 W(x) = 0 \quad (4)$$

$$\text{Where, } \beta^4 = \frac{\omega^2 m}{EI} \quad 0 < x < l$$

The Solution of the equation (4) is

$$W(x) = c_1 \sin \beta x + c_2 \cos \beta x + c_3 \sinh \beta l + c_4 \cos \beta l - \quad (5)$$

The constants of Equation (5) are obtained by applying boundary conditions and the expressions for natural frequency of the first four modes are given by,

$$\begin{aligned} \omega_1 &= 1.875^2 \sqrt{\frac{EI}{\rho AL^4}} \text{ rad/sec} \\ \omega_2 &= 4.694^2 \sqrt{\frac{EI}{\rho AL^4}} \text{ rad/sec} \\ \omega_3 &= 7.854^2 \sqrt{\frac{EI}{\rho AL^4}} \text{ rad/sec} \\ \omega_4 &= 10.995^2 \sqrt{\frac{EI}{\rho AL^4}} \text{ rad/sec} \end{aligned} \quad (6)$$

Impulse Technique

Figure 2 Shows the block diagram of instrumentation used for Impulse Technique. The accelerometer [Bruel and Kjaer 4374] was used to measure the acceleration through the charge amplifier [Bruel and Kjaer Type 2626] and the response was

recorded on the Dynamic Signal Analyzer [Agilent 35670A]. The specimens were excited using the Modally Tuned Impact Hammer [RION PH 7117]. This hammer was supplied with impact tip of varying hardness. It was observed that for the higher frequencies the harder tip was required to ensure a reproducible tip displacement vibration. The Dynamic Signal Analyzer (DSA) was used to store the output from the accelerometer and the force hammer. Fast Fourier Transform (FFT) of the time signal was obtained using the DSA. 16 averages were used to plot the Frequency Response Function [FRF] of the time signal.

Typical FRF obtained from the Hammer Impact Test are shown in Fig. 3. The series of the peaks in the FRF shows the natural frequencies of the beam. The damping factor for the materials is obtained using the half-power bandwidth method. The expression for damping factor ζ by the half-power band width technique is given by [15],

$$\zeta = \frac{\Delta\omega}{2\omega_n} \tag{7}$$

where,

$\Delta\omega$ = Band width at the half- power points of resonant peak for nth mode

ω_n = Resonant frequency

The half-power points are found at 3dB below the peak value of the FRF for the particular mode when the logarithmic scale is used or at $\frac{1}{\sqrt{2}}$ of this peak value when linear scale is used (Refer Fig. 4).

Logarithmic Decrement Method

The experimental set-up for the Sinusoidal technique is shown in Fig. 5. This technique is used to measure the rate at which the vibration amplitude decays and to compute the structural damping factor. The Modal exciter [National Aerospace Laboratories, Bangalore] and Accelerometer [Bruel and Kjaer 4374] were used for the vibration excitation and detection of the tip displacement of the beam respectively. The sine wave signal from the waveform generator [Hewlett Packard 33120A] was supplied to drive the modal exciter to excite the cantilever beam specimen into flexural response. Resonance was determined by monitoring the amplitude of the

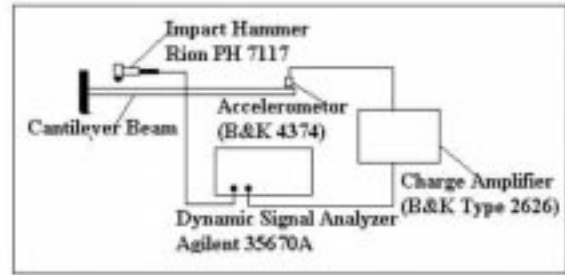


Fig. 2 Block diagram for Hammer Impulse Technique

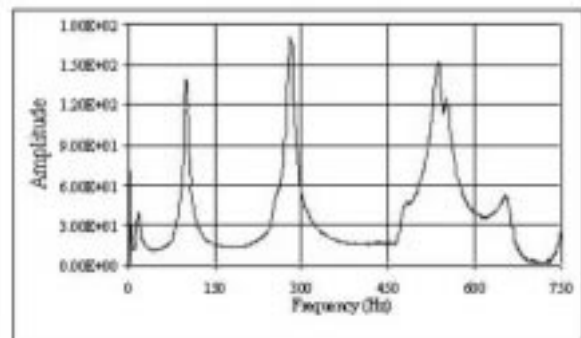


Fig. 3 Typical FRF obtained from Hammer Impulse Technique

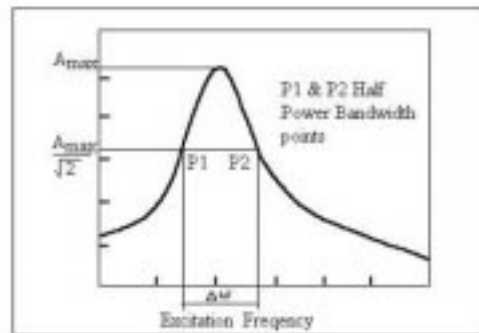


Fig. 4 Hammer impulse technique half power bandwidth damping factor measurement

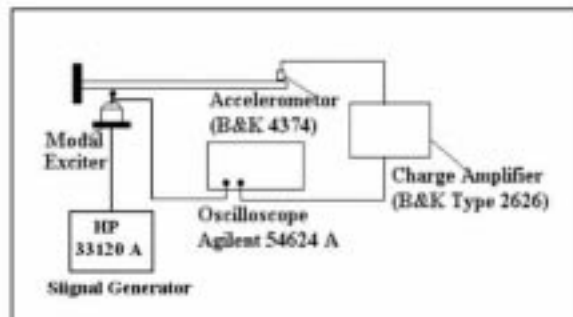


Fig. 5 Schematic of typical modal exciter set-up

oscillation on the Oscilloscope [Agilent 54624A] and was determined when this value reached maximum. Once the resonance was achieved, excitation signal to the modal exciter was disconnected freely.

The decay amplitude recorded with higher sampling rate in the Oscilloscope are shown in Fig. 6. It gives the two experimental amplitude data points as in Fig. 7 which are used to calculate the damping factor of the nanocomposite specimens. Damping factor in the Logarithmic decrement method is obtained by using the expressions [16],

$$\zeta = \frac{\delta^2}{\sqrt{4\pi^2 + \delta^2}} \quad \text{and}$$

$$\delta = \frac{1}{n} \ln \left(\frac{x_1}{x_{n+1}} \right) \quad (8)$$

Where,

- ζ = Damping factor,
- n = Number of cycles
- δ = Logarithmic decrement,

and x_1, x_{n+1} are the two displacement values at time intervals t_1 and t_2

In this method we need two experimental data values from the amplitude decay curve for calculation of damping factor. Therefore by increasing the data points between the two values the random error of the resultant-damping factor is reduced.

Result and Discussion

Structure and Morphology

The X-ray scattering intensity patterns for the UMT and MMT clay are shown in Fig. 8. The d-spacing was calculated from peak positions using the Bragg's Law $d = \lambda / (2 \sin \theta)$. Where d is the interlayer spacing distance, θ is the diffraction angle and λ is the X-ray wave length ($\lambda = 1.5408 \text{ \AA}$). In the XRD pattern for the un- modified and organically modified MMT, the characteristic peaks correspond to the basal spacing are 1.33nm and 1.69nm respectively. The XRD patterns of cured samples are shown in Figs. 9 and 10. It is seen that there is no characteristic peak of the UMT and

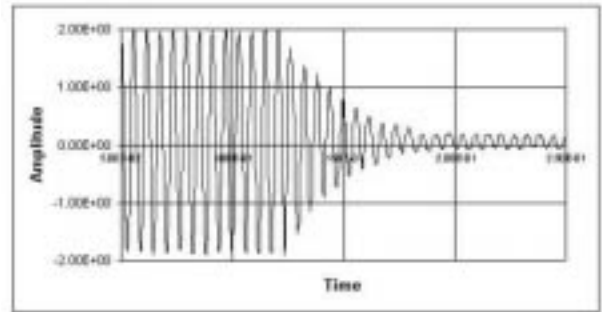


Fig. 6 Typical damping curve after excitation is stopped

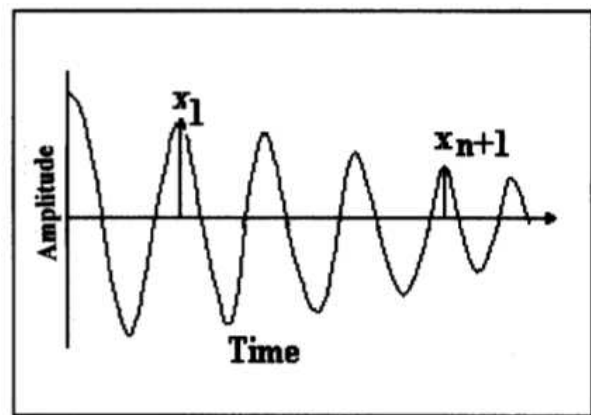


Fig. 7 Logarithmic decrement method – Free decay amplitude measurement of damping factor

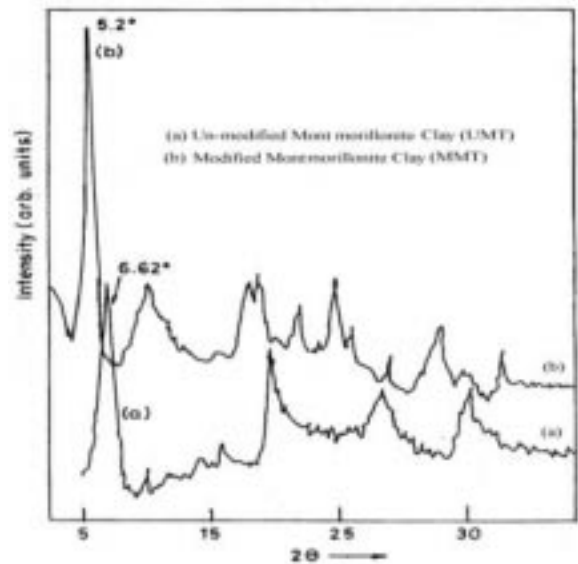


Fig. 8 XRD pattern of UMT and MMT clay

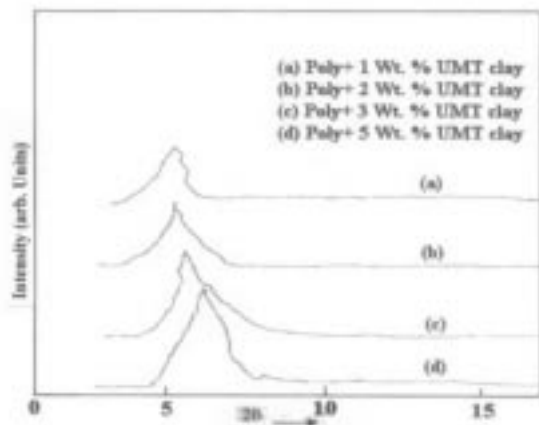


Fig. 9 XRD Patterns of Un-modified clay nanocomposite series

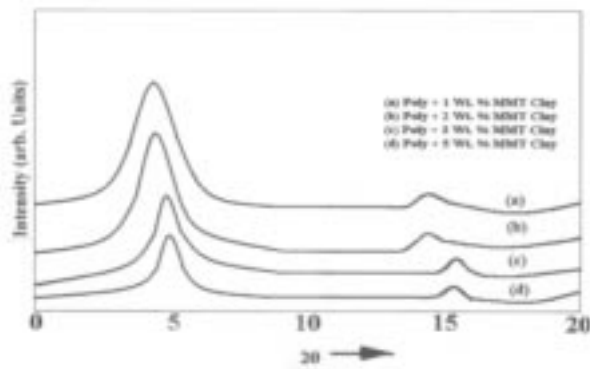


Fig. 10 XRD Patterns of modified clay nanocomposite series

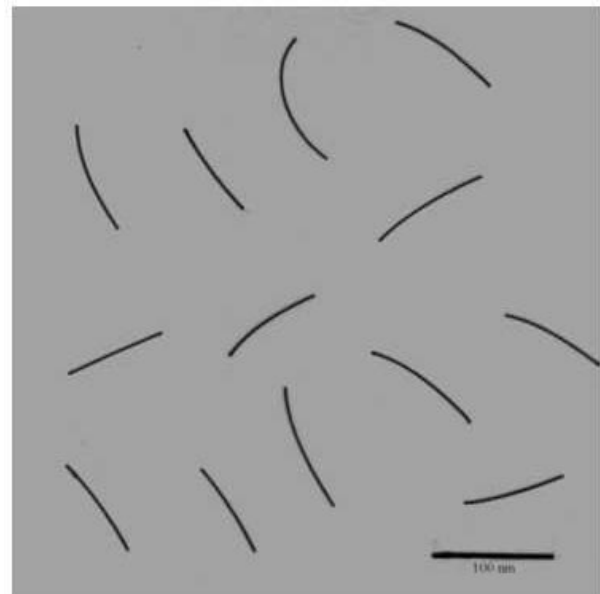


Fig. 11 TEM observation of Polyester+ 2wt. % modified clay nanocomposites

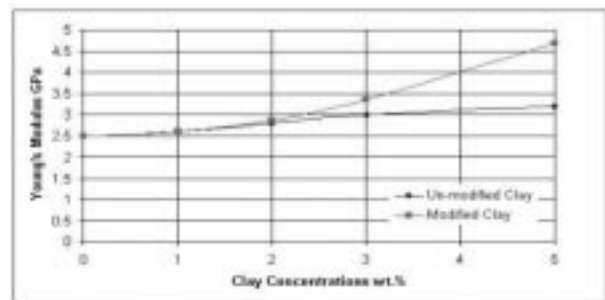


Fig. 12 Influence of UMT and MMT clay on Young's modulus

| Sl. No. | Wt. % of Clay | Interlayer d-spacing distance (Å) | |
|---------|---------------|-----------------------------------|-------------------------|
| | | UMT Clay nanocomposites | MMT Clay nanocomposites |
| 1 | 1 | 16.35 Å | 23.23 Å |
| 2 | 2 | 16.35 Å | 22.07 Å |
| 3 | 3 | 15.22 Å | 18.39 Å |
| 4 | 5 | 14.25 Å | 17.65 Å |

MMT for different Wt. % of clay, confirming the formation of nanocomposites. The d- spacing distances calculated from peak positions are shown in Table 1. The cross linked polyester chain into the galleries of UMT clay increases the d-spacing to 1.63nm for 1Wt. % and 1.42nm for 5Wt. % of clay samples, where as in modified MMT it is 2.32nm for 1Wt. % clay and 1.79nm 5Wt. % of clay. The increase in the d-spacing of

the composites shows that the polyester matrix is successfully gone into the galleries of un- modified and organically modified MMT clay platelets to form intercalated nanocomposites.

More direct evidence of the formation of nanocomposites is provided by the TEM images. TEM picture of 2 Wt. % of MMT clay nanocomposites will be as shown in the Fig. 11. The dark lines of black color are intersection of clay layers of 1nm thickness and the spaces between the dark lines are called interlayer distance of Montmorillonite. The light grey spaces between the interlayer are called matrix. The TEM photograph proves the successful insertion of the matrix between the gallery spaces of Montmorillonite clay.

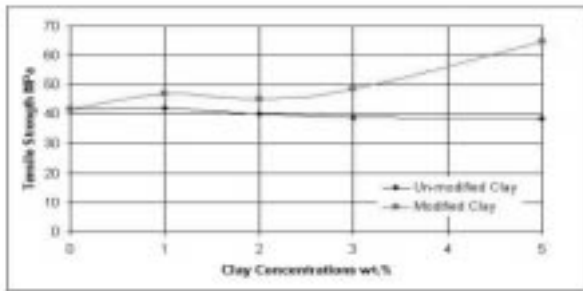


Fig. 13 Influence of UMT & MMT clay on Tensile

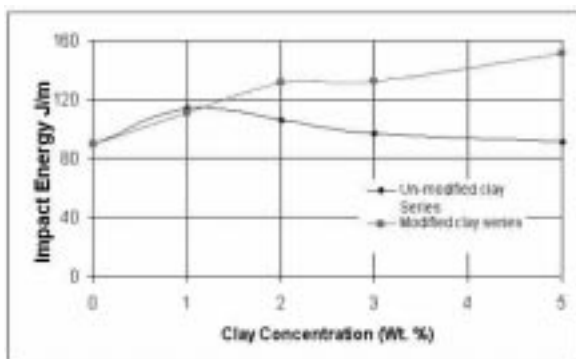


Fig. 14 Influence of UMT & MMT clay on Impact energy of polyester clay nanocomposite

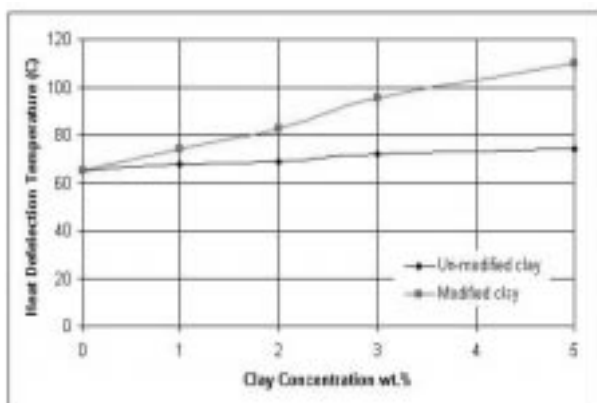


Fig. 15 Influence of UMT & MMT clay on Heat deflection Temperature (HDT)

Mechanical Properties

Young's Modulus

The values of Young's Modulus of the UMT and MMT clay reinforced nanocomposites are shown in Fig. 12. The Young's Modulus of MMT increases with increase of clay content. In MMT clay the increase in tensile modulus is about 43% at 5 Wt. % of clay

content. The improvement of Young's Modulus is due to intercalation and good dispersion of clay particles that restrict the mobility of the polymer chains under loading as well as good interfacial adhesion between the particles and the polyester matrix. It is seen that the modulus of the organically modified MMT clay nanocomposites is higher than that of the un-modified clay nanocomposites. In un-modified MMT the increase in modulus is 28% for 5 Wt. % of clay content as compared with neat polymers. In UMT, there is little increase in intercalation/exfoliation between the layers and hence the increase in the modulus values is also less.

Tensile Strength

The tensile strength measured from the tensile tests of UMT and MMT clay reinforced nanocomposites are shown in Fig. 13. The platelet alignment of clay in polymer matrix contributes to the improvement in the tensile strength of nanocomposites. The tensile strength of nanocomposites is seen to increase with increase of clay content and 55% increase is seen in specimens, whereas the increase in tensile strength of UMT clay composites is very less. For higher clay concentration of UMT, the clay particles act as stress concentrators and tend to reduce the strength of the materials. At higher loading there is a low degree of clay-polymer interaction, resulting in interfacial debonding and thus reducing the tensile strength.

Izod Impact Energy

The Izod impact experimental results for PCN are shown in Fig. 14. It is seen that the impact behaviour is improved with increase of MMT clay content. There is an increase of 68.27% for 5 Wt. % of MMT clay concentration. In UMT the improvements are noted at the lower concentrations (2Wt. %) and gets gradual decrement with further clay addition. However, it remains above the performance of the neat resin for clay upto 5%.

The ineffective intercalation and agglomeration in higher volume content of UMT clay serve as the stress concentrators and hence there is reduction in the performance. In MMT there is well formed intercalation of nanocomposites even at higher volume % and hence there is increase in impact strength.

Heat Deflection Temperature (HDT)

The Heat Deflection Temperature (HDT) is a measure of polymer resistance to distortion under a given load at elevated temperature. The value obtained

for a specific polymer grade depends on the base resin and the presence of reinforcing agents. The results obtained from this test are shown in Fig. 15, which imply that the reinforcement effect of MMT clay increases the HDT of the nanocomposites whereas the UMT clay has no influence in HDT.

Dynamic Mechanical Analysis

Since DMA is very sensitive to physical and chemical structure of polymers over a wide range of temperatures, it is used to study the storage modulus, loss modulus, loss tangent and glass transition temperature. The experimental results of DMA conducted on UMT samples are shown in Fig. 16. The storage modulus gradually increases up to 2Wt. % and decreases on further addition of clay. The Loss tangents against the temperature range are showed in Fig 17. The peak shown in the loss tangent curve gives the glass transition temperature (T_g) and it is almost the same.

The frequency dependent storage modulus (E') and loss modulus (E'') values are increasing monotonically with increase of MMT clay which are shown in Fig. 18. Virgin polyester shows storage modulus E' of 5500 MPa at room temperature. The reinforcing effect of clay increases E' up to 7900MPa for 5Wt. % clay showing about ~43% increase. The MMT nanocomposites show the storage modulus higher than the matrix, over a wide temperature range, with increasing clay concentrations. The increase in storage modulus (E') is due to the dispersion of clay in the polymer matrix.

The $\tan \delta$ versus temperature scale, occurring between 30°C to 180°C for different clay concentrations of MMT are shown in Fig. 19. The vicinity of damping peak seen from the figure shows that the clay reinforcement results in high damping of the material. There is a clear peak at ~88°C for pure polyester which is glass transition temperature. For 5Wt. % clay it occurs at 110°C.

After the glass transition temperature the variation of storage modulus is constant for all weight percentages of clay but the clay concentration broadens the peak for increase in Wt. % of clay.

Natural Frequency

The Experimental results of the natural frequency of PCN specimens for UMT clay with different Wt. % are given in Tables-2 to 5. The gradual improvement in the natural frequency is noticed with increase of clay content. It is seen from Tables-6 to 9 that reinforcement

Table-2: First mode Natural frequency: UMT clay nanocomposites

| Specimen Name | Wt. % of UMT Clay | Mode I Natural frequency (Hz) | |
|---------------|-------------------|-------------------------------|--------|
| | | Experimental | Theory |
| POU00 | 0 | 20.80 | 19.39 |
| POU01 | 1 | 19.75 | 19.26 |
| POU02 | 2 | 21.00 | 20.02 |
| POU03 | 3 | 21.25 | 20.81 |
| POU05 | 5 | 22.00 | 21.26 |

Table-3: Second mode Natural frequency: UMT clay nanocomposites

| Specimen Name | Wt. % of UMT Clay | Mode II Natural frequency (Hz) | |
|---------------|-------------------|--------------------------------|--------|
| | | Experimental | Theory |
| POU00 | 0 | 97.50 | 121.56 |
| POU01 | 1 | 101.25 | 126.73 |
| POU02 | 2 | 110.50 | 125.49 |
| POU03 | 3 | 119.25 | 130.43 |
| POU05 | 5 | 126.00 | 133.30 |

Table-4: Third mode Natural frequency: UMT clay nanocomposites

| Specimen Name | Wt. % of UMT Clay | Mode III Natural frequency (Hz) | |
|---------------|-------------------|---------------------------------|--------|
| | | Experimental | Theory |
| POU00 | 0 | 292.00 | 340.49 |
| POU01 | 1 | 278.7 | 338.19 |
| POU02 | 2 | 291.25 | 351.52 |
| POU03 | 3 | 287.75 | 365.34 |
| POU05 | 5 | 307.50 | 373.39 |

Table-5: Fourth mode Natural frequency: UMT clay nanocomposites

| Series | Wt. % of MMT Clay | Mode I Natural frequency (Hz) | |
|--------|-------------------|-------------------------------|--------|
| | | Experimental | Theory |
| POU00 | 0 | 377.00 | 668.76 |
| POU01 | 1 | 375.00 | 662.44 |
| POU02 | 2 | 391.25 | 688.56 |
| POU03 | 3 | 473.75 | 715.62 |
| POU05 | 5 | 540.00 | 731.40 |

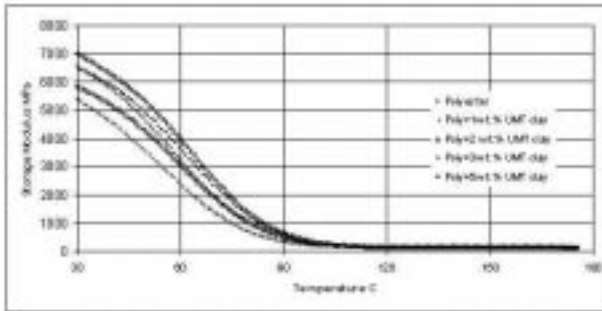


Fig. 16 Storage modulus of UMT clay nanocomposites series

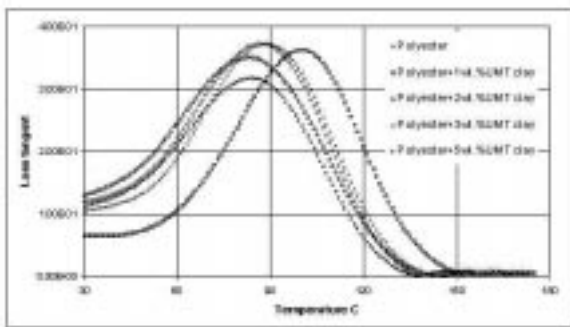


Fig. 17 Loss tangent of UMT clay nanocomposites series

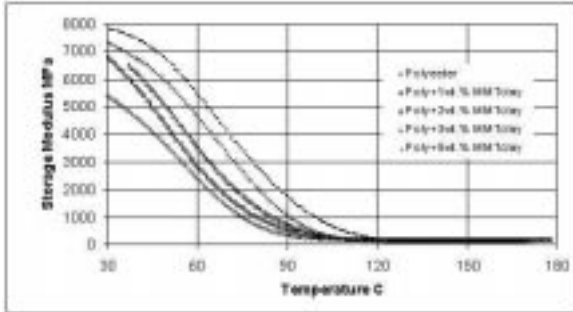


Fig. 18 Storage modulus of MMT clay nanocomposites

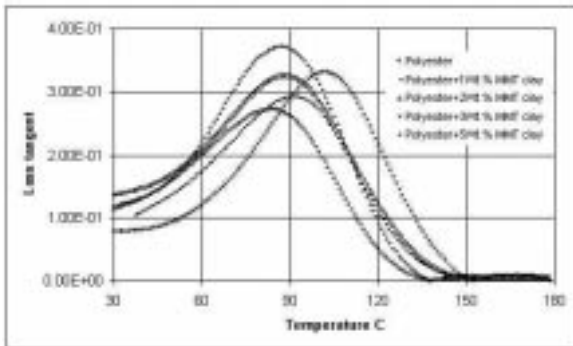


Fig. 19 Loss Tangent of MMT clay nanocomposites

Table-6: First mode Natural frequency: MMT clay nanocomposites

| Series | Wt. % of MMT Clay | Mode I Natural frequency (Hz) | |
|--------|-------------------|-------------------------------|--------|
| | | Experimental | Theory |
| POC00 | 0 | 20.8000 | 19.39 |
| POC01 | 1 | 20.9400 | 18.43 |
| POC02 | 2 | 19.1000 | 19.32 |
| POC03 | 3 | 21.6000 | 23.32 |
| POC05 | 5 | 25.9900 | 27.51 |

Table-7: Second mode Natural frequency: MMT clay nanocomposites

| Series | Wt. % of MMT Clay | Mode II Natural frequency (Hz) | |
|--------|-------------------|--------------------------------|--------|
| | | Experimental | Theory |
| POC00 | 0 | 118.500 | 121.52 |
| POC01 | 1 | 116.940 | 115.52 |
| POC02 | 2 | 119.500 | 121.09 |
| POC03 | 3 | 152.500 | 146.16 |
| POC05 | 5 | 164.000 | 172.41 |

Table-8: Third mode Natural frequency: MMT clay nanocomposites

| Series | Wt. % of MMT Clay | Mode III Natural frequency (Hz) | |
|--------|-------------------|---------------------------------|--------|
| | | Experimental | Theory |
| POC00 | 0 | 248.00 | 340.39 |
| POC01 | 1 | 261.30 | 323.58 |
| POC02 | 2 | 242.00 | 339.18 |
| POC03 | 3 | 246.00 | 409.39 |
| POC05 | 5 | 352.00 | 482.94 |

Table-9: Fourth mode Natural frequency: MMT clay nanocomposites

| Series | Wt. % of MMT Clay | Mode IV Natural frequency (Hz) | |
|--------|-------------------|--------------------------------|--------|
| | | Experimental | Theory |
| POC00 | 0 | 453.200 | 625.34 |
| POC01 | 1 | 464.220 | 633.90 |
| POC02 | 2 | 479.214 | 664.44 |
| POC03 | 3 | 513.540 | 801.45 |
| POC05 | 5 | 602.200 | 958.40 |

of the MMT clay shifts the natural frequency to higher values for all modes of vibration. The 25 % increase in natural frequency is obtained in the first mode and 39%, 42% and 33% improvements are obtained for second, third and fourth mode respectively. The good dispersion of the nano-clay increases the stiffness of the material and hence there is an increase in the natural frequency.

The theoretical values obtained by Euler-Bernoulli Beam theory are given in Tables 2 to 9. The natural frequencies computed by theory have good agreement for first two modes. In higher modes, experimental values do not match well with theoretical values which require further investigation of modulus values obtained from both experiments and theory.

Damping Factor

The damping factor determined by Hammer Impulse and Logarithmic Decrement Method experiments for different UMT clay concentrations corresponding to the first four modes are shown in Figs. 20 to 23. It is seen that there is improvement in damping for lower concentrations (up to 2 Wt. %) and then it decreases with further increase of clay.

The damping effect of the MMT clay in the polyester matrix is shown in Figs. 24 to 27. As the clay concentration increases, the damping factor also increases for all modes. The platelet structure in the polymer matrix results in the improvement of first mode of damping factor by 79% whereas it is 52%, 30%, and 65.40% for second, third and fourth modes respectively. These improvements are due to large surface area of platelet structure. The polymer chain inserted into the host galleries of the clay provides superior energy dissipative characteristics thus the clay serves as the damping medium in the polyester resin providing better dynamic characteristics. The small dispersion in the damping values obtained between IH and LD may be due to the presence of shaker which remains in contact with the specimen during decay, after the signal is cut off.

Conclusions

Two classes of PCN were prepared in polymer matrix with reinforcement of UMT and MMT clay at different concentrations. The formation of nanocomposites was confirmed by XRD diffraction test and TEM. The reinforcing effect of MMT clay enhances the modulus by 43% and the tensile strength is increased by 55% for 5 wt. % of the clay where as the improvement is less in the UMT clay nanocomposites.

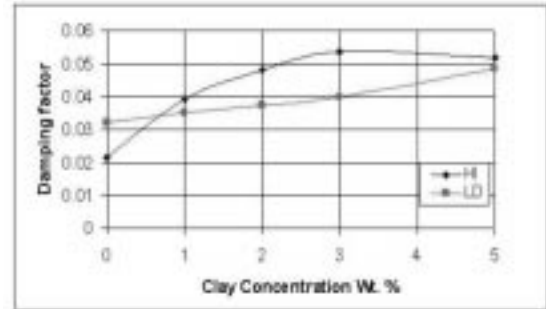


Fig. 20 Influence of UMT clay on First mode damping factor

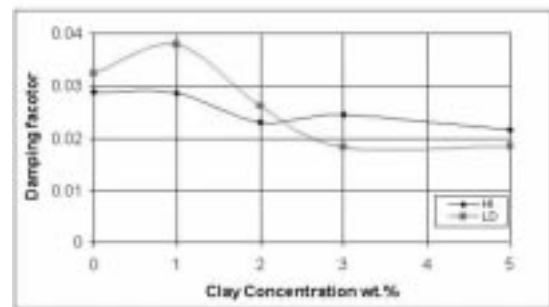


Fig. 21 Influence of UMT clay on Second mode damping factor

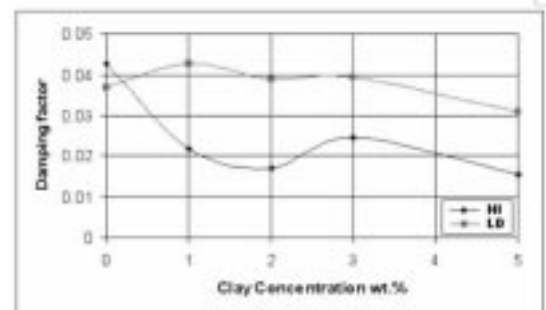


Fig. 22 Influence of UMT clay on Third mode damping factor

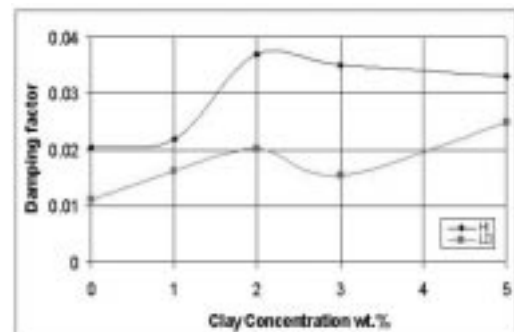


Fig. 23 Influence of UMT clay on Fourth mode damping factor

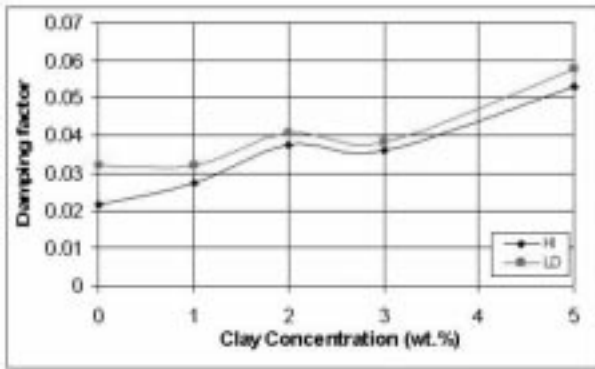


Fig. 24 Influence of MMT clay on First mode damping factor

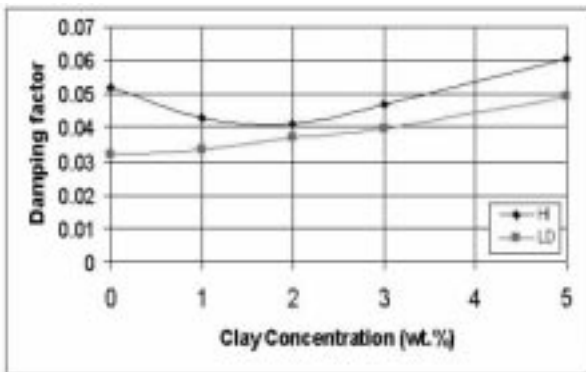


Fig. 25 Influence of MMT clay on Second mode damping factor

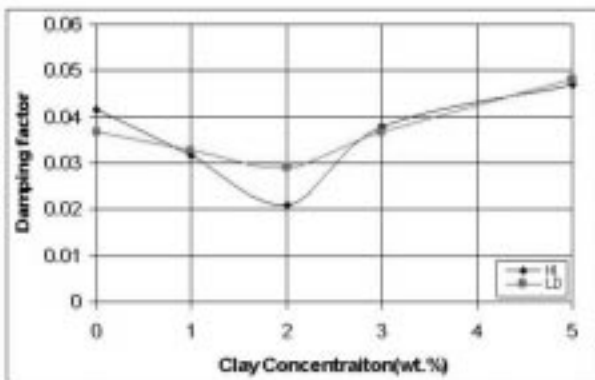


Fig. 26 Influence of MMT clay on Third mode damping factor

The impact energy and Heat Deflection Temperature (HDT) are increased by 68.27% and 25 % for MMT clay nanocomposites.

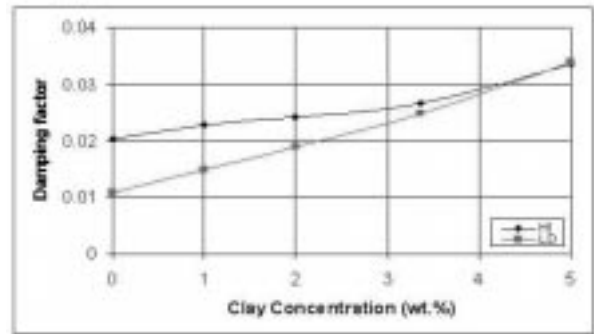


Fig. 27 Influence of MMT clay on Fourth mode damping factor

In MMT clay nanocomposites there is progressive increase in storage modulus and loss factor with increasing clay concentration showing excellent energy dissipative capability and damping properties. The UMT clay composites enhance the storage modulus and Loss tangent at lower Wt. % and then decrease with increase of clay content. The natural frequency and damping factor are computed for various Wt. % of clay by Impulse Technique and Logarithmic decrement method. There is improvement in damping properties for lower Wt. % of UMT clay whereas in MMT clay nanocomposites, the properties have increased with increase of clay content, which provides superior dynamic characteristics.

References

1. Pinnavaia, T.J. and Beall. Eds. G.W., "Polymer-Clay Nanocomposites", John Wiley and Sons Limited, New York, 2000.
2. Lebaron, P.C., Wang, Z. and Pinnavaia, T.J., "Polymer Layer Silicate Nanocomposites: An Overview", Applied Clay Science 15, pp.11-29, 1999.
3. Michale Alexandre. and Philippe Dubois., "Polymer-Layered Silicate Nanocomposites: Preparation, Properties and uses of a New Class of Materials", Material Science and Engineering 28, pp.1-63, 2000.
4. Blumstein, A., "Polymerization of Adsorbed Monolayer: II. Thermal degradation of the Inserted Polymer", Journal of Polymer Science, A3, pp.2665-2673, 1995.

5. Vaia, R.A., Price, G., Ruth, P.N., Nguyen, H.T. and Lichtenhan, J., "Polymer/Layered Silicate Nanocomposites as High Performance Ablative Materials", *Applied Clay Science*, 15, pp.67-92, 1999.
6. Kathleen Carrado, A., "Synthetic Organo and Polymer Clays: Preparation, Characterization and Material Application", *Applied Clay Science*, 17, pp.1-23, 2000.
7. Kornmann, X. and Berglund L.A., "Nanocomposites Based on Montmorillonite and Un-saturated Polyester", *Polymer Engineering. Science*, 38, pp.1351-1358, 1998.
8. Suh, D.J., Lim. Y.J. and Park, O.O., "The Property and Formation Mechanism of Un-saturated Polyester-Layered Silicate Nanocomposite Depending on the Fabrication Methods", *Polymer Engineering Science*, 41, pp.8557-8563, 2000.
9. Bharadwaj, R.K., Mehrabi, A.R., Hamilton, C., Trujillo, C., Muruga, M., Fan, R., Chavira, A. and Thomson, A.K., "Structure-Property Relationships in Cross-Linked Polyester-Clay Nanocomposites", *Polymer*, 43, pp.3699-3705, 2002.
10. Baran, A., Inceoglu. and Ulku Yilmazer, "Synthesis and Mechanical Properties of Unsaturated Polyester based Nanocomposites", *Polymer Engineering and Science*, 43, pp.661-669, 2003.
11. Robert, D Adams. and Bacon, D.G.C., "The Dynamic Properties of Unidirectional Fibre Reinforced Composites in Flexure and Torsion", *Journal of Composite Materials*, 7, pp.53-67, 1972.
12. Nelson, D.J., "Dynamic Testing of Discontinuous Fibre Reinforced Composite Material", *Journal of Sound and Vibration*, 64(3), pp.403-419, 1979.
13. Gill, P.S., "Dynamic Mechanical Analysis of Advanced Composites", *Composite Structures*, 2, pp.235-243, 1984.
14. Ioana C. Finegan. and Ronald F. Gibson, "Recent Research on Enhancement of Damping in Polymer Composites", *Composite Structures*, 44, pp.89-98, 1999.
15. Suarez, S.A., Gibson, R.F. and Deobald, L.R., "Random and Impulse Technique for Measurement of Damping in Composite Materials", *Experimental Technique*, October, pp.19-24, 1984.
16. Wren, G.G. and Kinra, V.K., "An Experimental Technique for Determining a Measure of Structural Damping", *Journal of Testing and Evaluation*, 16(1), pp.77-85, 1988.